JOURNAL OF MATERIALS SCIENCE 19 (1984) 1548–1555

X-ray microanalysis and acoustic emission studies on the formation mechanism of secondary cracks in PMMA

KAZUMI MATSUSHIGE*, YASUHIRO SAKURADA, KIYOSHI TAKAHASHI
Research Institute for Applied Mechanics, Kyushu University, Kasuga 816, Japan

The formation mechanism of secondary cracks in poly(methyl methacrylate) (PMMA) was investigated using various methods. X-ray element analysis and SEM observations on parabolic markings showed that there exist certain defects such as silicon compound and microcracks at their foci, forming the potential sources for the secondary cracks (a static factor). On the other hand, the fracture process was monitored simultaneously with acoustic emission (AE) and high speed shadow-optical techniques. These observations revealed that density of the parabolic marking has a closer correlation to the amplitude of the stress wave emitted during crack propagation, rather than to the values of crack speed or stress intensity factor (a dynamic factor). The formation mechanism is thus explained by the combination of these static and dynamic factors.

1. Introduction

Examination of fracture surfaces (fractography) provides a variety of information about fracture processes of tested materials. Parabolic or conic markings commonly seen on the fracture surfaces of PMMA are the classically and most widely studied ones [1–7]. These markings are produced by the intersection of a main crack front with a radially propagating secondary crack front. The secondary cracks are believed to be initiated from some local flaws ahead of the primary crack. However, the nature of the flaws have not been definitely elucidated yet. Electron microscopy in a focus region of parabolic markings mostly gives featureless images, which suggests that the size of the flaws or defects may be gauged by a molecular scale. In fact, from experimental findings that the density of parabolic markings increased with decreasing molecular weight of PMMA samples, Newman and Wolock [5] suggested that the origin of the secondary crack might be associated with some structural discontinuities arising from molecular chain ends.

From a viewpoint of fracture mechanics, Cotterell [6] reported that the density of parabolic markings is proportional to the fracture toughness, and suggested that the secondary cracks start from the crazed region ahead of the primary fracture front. On the other hand, as to the influence of stress waves on the fracture morphology in PMMA several discussions have recently been given. Kusy and Turner [8] indicated that the stress waves affect the disposition of rib markings. Doyle [9] suggested that the so-called "mackerel pattern" arises from structural weakness or actual interfacial fracture caused by the propagation of stress waves along the craze–bulk boundaries. However, as to the contribution of the stress waves to the secondary crack initiation process few works seems to have been performed.

In this study, the formation mechanism of the secondary cracks was investigated from both static and dynamic viewpoints. First, in order to elucidate the impurities at foci of parabolic markings, and also to examine their fracture morphology, an electron microprobe X-ray analyser

*Present address: Department of Applied Science, Faculty of Engineering, Kyushu University, Fukuoka 812, Japan.

0022–2461/84 $03.00 + .12

(EPMA) was employed. Second, high speed shadowgraphy and AE measurements were simultaneously carried out during crack propagation for studying dynamic factors affecting initiation of the secondary cracks.

2. Experimental details

Tensile specimens were cut from commercial cast sheets of PMMA (Mitsubishi Rayon, Acrylite-S). They had a geometry of 200 mm in length, 40 mm in width and 5 mm in thickness. In order to obtain a wide range of crack velocities, the following three types of single-edge notches were introduced; (a) pre-cracked (fatigue) notches, (b) V-shaped notches and (c) drill-holed notches. Specimens were loaded in an Instron-type tensile machine at various crosshead speeds and at room temperature.

Fracture surfaces were decorated with gold or carbon and then examined in an EPMA (Shimadzu, EMX-SM) apparatus. Scanning electron microscopy (SEM) as well as X-ray microanalysis of impurities in a focus region of each parabolic marking were performed. The spacial resolution of the apparatus was as high as 20 nm, whereas impurities of 0.001% (10^{-17} g) in weight could be detected. However, because the apparatus was a conventional wavelength dispersive type, elements for analysis had to be selected individually. Delicate materials such as polymers could easily be damaged by intense electron beam currents (of the order of 100 to 1000 nA), which caused contamination within the EPMA apparatus. It seems that these difficulties have prevented researchers from systematic EPMA studies on the origin of secondary cracks.

The fracture propagation process was monitored with both a Cranz–Schardin camera and an AE system. Fracture velocities as well as mode I stress intensity factor were determined by high speed photography. For determining the mode I stress intensity factor, a shadow optical (caustics) method [10] was used. A dynamic stress optical constant of 0.49×10^{-10} m^2 N^{-1} [10] was adopted in the present determination. Details of the caustics experiments are given, for example, in [11]. Simultaneously with high speed photography, the stress waves emitted from a propagating crack was detected by an AE system, as shown in Fig. 1. The resonance frequency of the transducer was 140 kHz, whereas the high-pass filter had the minimum pass frequency of 20 kHz.

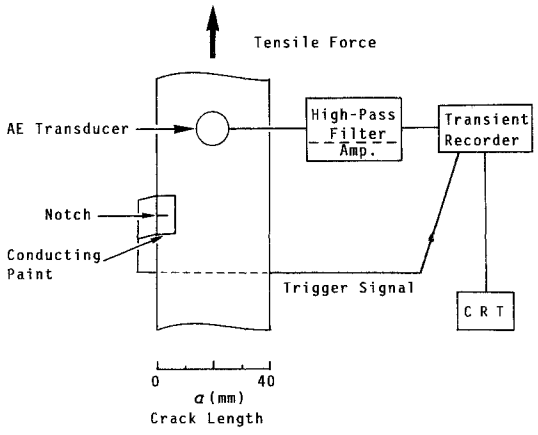

Figure 1 Schematic diagram for AE measurements.

AE signals were once stored in a digital transient recorder and then displayed on a CRT. Trigger pulses for the high speed camera as well as for the transient recorder were obtained by the conducting line method.

3. Results and discussion

3.1. EPMA observations

A great number of parabolic markings were examined in detail in their focus regions. The majority of them exhibited a featureless structure, as already reported by other investigators [3–5]. Exceptionally, however, several parabolic markings were found to exhibit certain defects at their foci, as shown in Fig. 2. These defects differed in each case; a microcrack is found in Fig. 2a, a tiny hollow and a projection is seen in Fig. 2b, and some foreign material is observed in Fig. 2c. These SEM pictures suggest that these defects, $1 \sim 3$ μm size, had already existed in the specimen material as crack nuclei.

In order to elucidate the origin of nuclei of the parabolic markings, especially those which exhibited a featureless structure at their foci, element analysis was carried out by the EPMA apparatus. Because several chemical compounds such as catalysts, accelerators, plasticizers and ultraviolet absorbers are commonly included in the specimen material during its polymerization and processing processes, these compounds were naturally thought to become their origins. Therefore, such elements as nitrogen, potassium, sulphur, sodium and iron, which should be contained in these additives were chosen for the present X-ray examination. Moreover, silicon was also searched for because it generally coexisted with metals

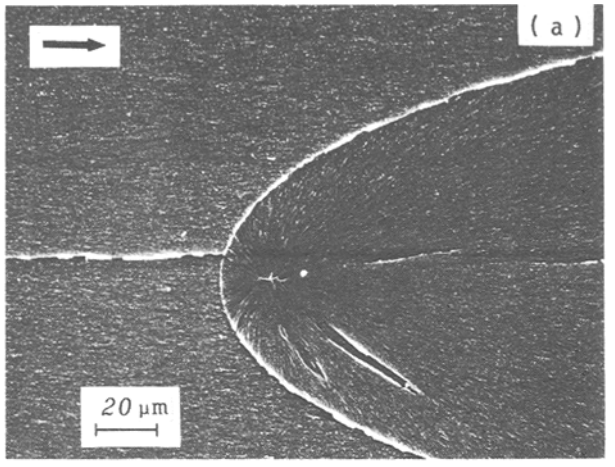

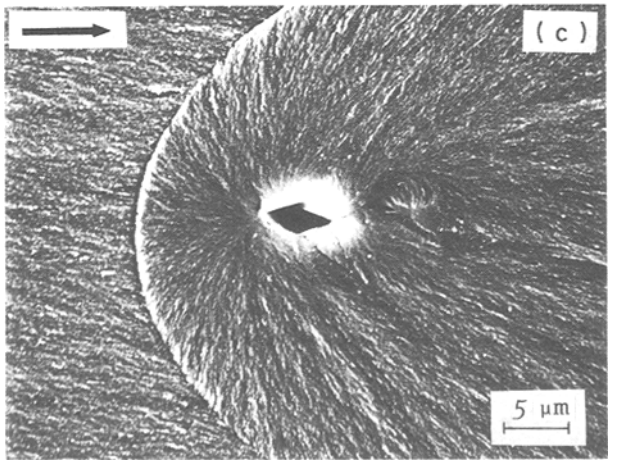

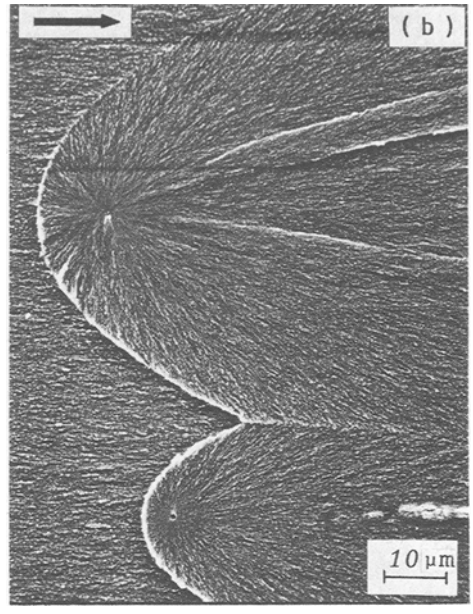

Figure 2 Scanning electron micrographs showing certain defects at the focus region of parabolic markings.

as an impurity. The experimental results are summarized in Table I. The former 5 elements were not detected, except only in one case for iron. Therefore, the additives mentioned above are considered, if present, to exist at an extremely low level, i.e. beyond the resolving power of this apparatus, and not to become a stress raiser for crack nucleation. Silicon, on the other hand, was found for five cases among 86 parabolic markings examined. Four cases out of the five exhibited the existence of silicon locally at the focus region, as typically shown in Fig. 3. In the figure, an X-ray line scan along a route (a) through the focus gave the maximum value of the X-ray intensity, while that along a route (b) off the focus showed no detectable X-ray. This suggests that in these cases a small silicon particle and/or its compounds acted as a stress raiser. In the remaining one case, in which the examination was performed for the secondary crack as already shown in Fig. 2c, silicon was detected not at the focus but in its surroundings as shown in Fig. 4. This figure presents a series of line analysis profiles for silicon X-rays, superimposed on the SEM picture of Fig. 2c. White ripple traces indicate noise level. At the very focus point, X-ray intensity was comparable to the noise level, whereas in a circular region of about 10 μm radius around the crack nucleus the silicon X-ray was detected. It seems

TABLE I Summary of X-ray element analysis in a focus region of parabolic markings

Element	Source compound	Examined number	Detected number
N	catalyst	69	0
K	catalyst	17	0
S	catalyst, accelerator	17	0
Na	catalyst, accelerator	17	0
Fe	accelerator	86	1
Si	dust, impurity	86	5

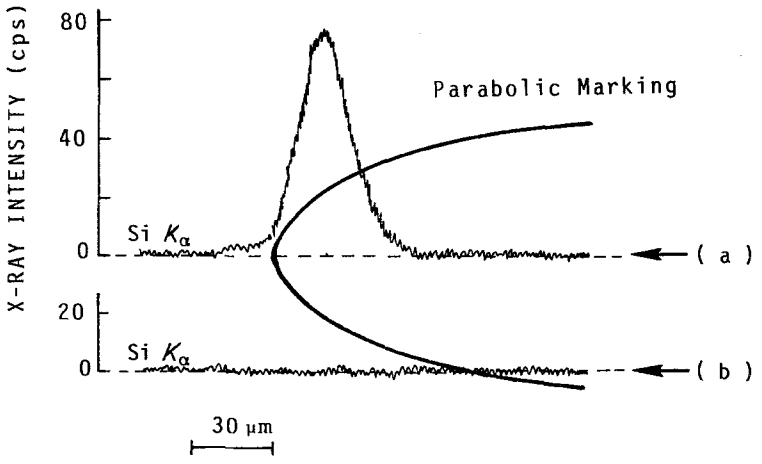

Figure 3 X-ray line analysis along different paths (a) and (b) through a parabolic marking.

that in this special case a foreign material, which was surrounded with silicon compounds, became a crack nucleus.

Thus, the results of SEM observation as well as X-ray analysis have revealed that in some cases there definitely existed certain defects such as microcracks, silicon compounds and other foreign materials at the focus region, although in many cases the origins of the secondary cracks could not be identified. These defects and unknown origins may be quite different in size as well as in quality. The existence of these stress raisers is thought to provide a "static factor" for secondary crack initiation. Furthermore, a "dynamic factor" is also considered to play an important role upon the initiation of the secondary crack, as discussed in the following section.

3.2. AE measurements and high speed shadowgraphy

Dynamic parameters which should affect and induce secondary crack initiation were investigated by AE measurements coupled with high speed shadowgraphy. Fig. 5 presents examples of AE signals and simultaneously taken high speed shadowgraphs for a fast crack. Numbers given in the AE oscillogram correspond to those in shadowgraphs. Numbers 1 to 3 are obtained from a crack propagation process, while number 4 corresponds to failure completion. Numbers 5 and 6 are obtained just after fracture, where the propagating caustics due to solitary surface waves are clearly visualized. The waves, travelling at a speed of about 1.1 km sec^{-1}, exhibited intense AE signals. On the other hand, AE signals in the stages 1 to 3

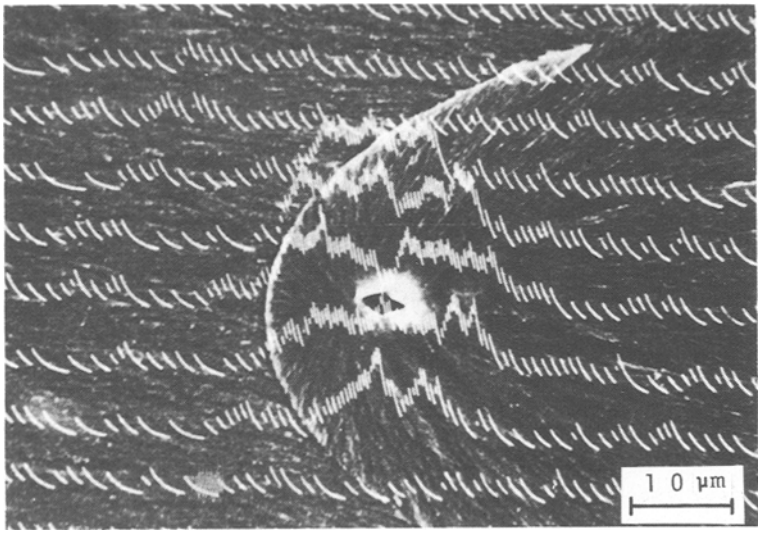

Figure 4 A series of X-ray line analysis profiles superposed on the micrograph, which is shown in Fig. 2c.

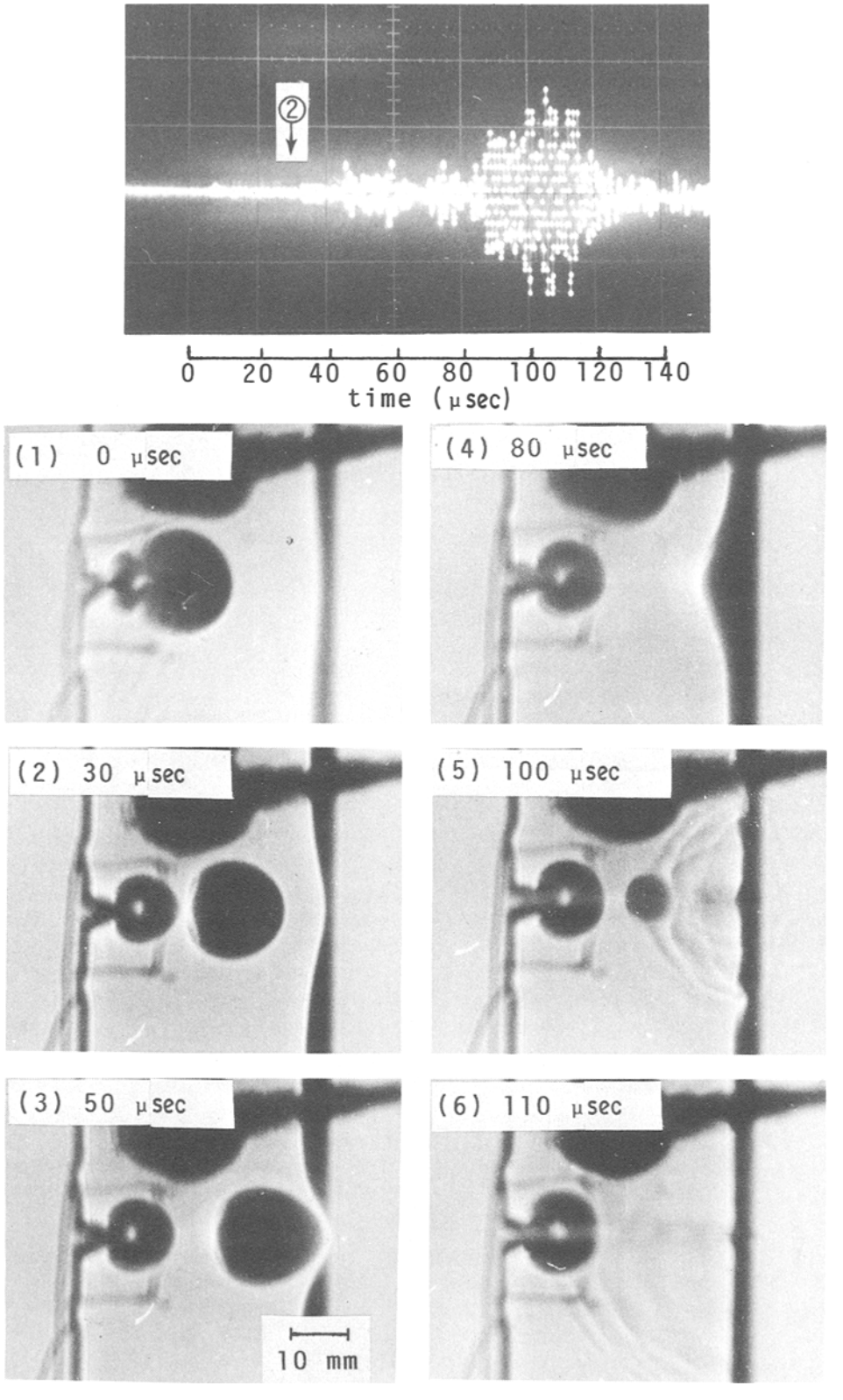

Figure 5 AE signals and high speed shadowgraphs simultaneously observed during a course of fracture. An AE transducer can be seen in the upper part of caustics.

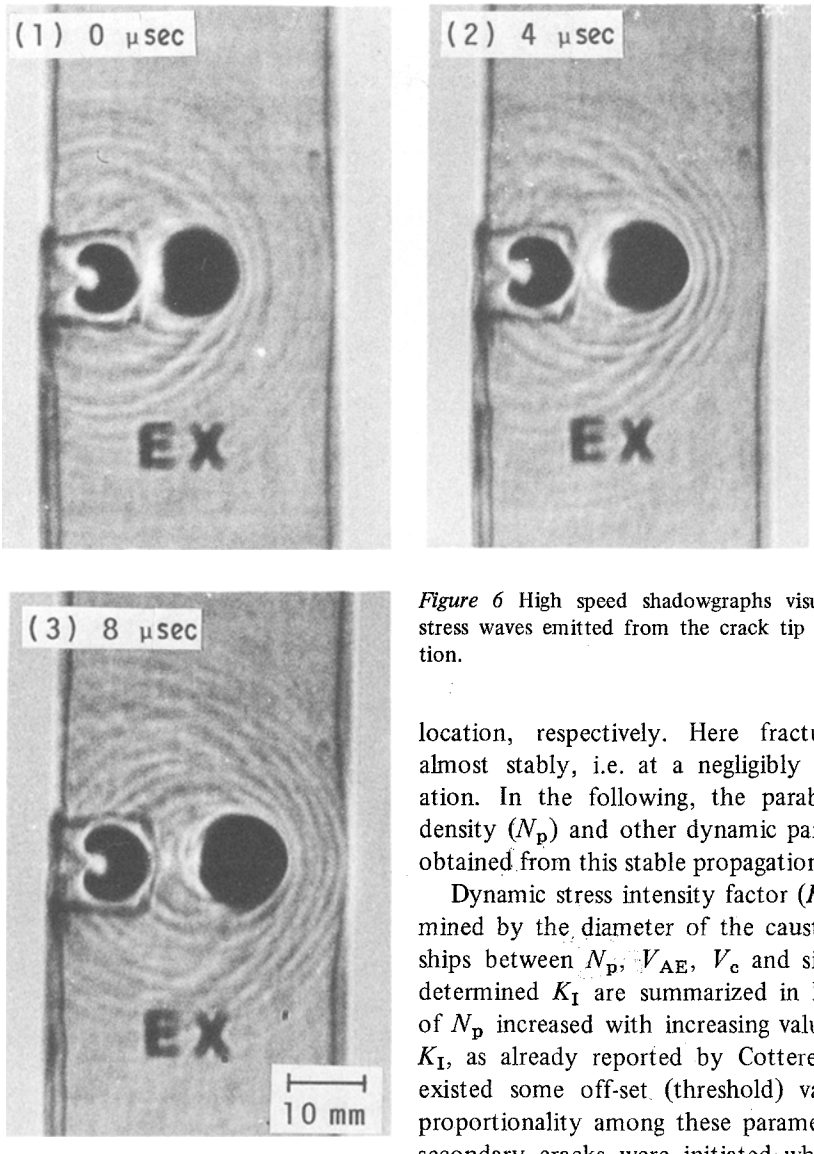

Figure 6 High speed shadowgraphs visualizing intense stress waves emitted from the crack tip during propagation.

showed a gradual increase from a low level in their intensity (V_{AE}) with the progression of the cracks. Although the existence of stress waves in the process of crack propagation was not clear in Fig. 5, they could be visualized when fracture velocity (V_c) became larger, as typically shown in Fig. 6, where the crack propagated at a velocity of about 500 m sec^{-1}. A number of shadowgraphs taken through the experiment showed that the higher the value of V_c is, the more clearly stress waves are visualized, which is in accord with the results obtained from AE measurements. Fracture surface morphology at various fracture velocities is shown in Fig. 7. Each value of V_c given in the figure indicates fracture velocity at each labelled location, respectively. Here fracture advanced almost stably, i.e. at a negligibly small acceleration. In the following, the parabolic marking density (N_p) and other dynamic parameters were obtained from this stable propagation area.

Dynamic stress intensity factor (K_I) was determined by the diameter of the caustics. Relationships between N_p, V_{AE}, V_c and simultaneously determined K_I are summarized in Fig. 8. Values of N_p increased with increasing values of V_c and K_I, as already reported by Cotterell [6]. There existed some off-set (threshold) values for the proportionality among these parameters. That is, secondary cracks were initiated when the values of V_c and/or K_I exceeded critical values, below which only the main cracks proceeded. From these results, one may postulate critical fracture velocity or critical stress intensity factor criterion. However, the experimental findings that values of V_{AE} showed a close correlation with values of N_p, suggests that AE waves could have considerable effect in initiation of the secondary fracture. This consideration may not be unnatural if we consider that multiple crack nucleation in PMMA can be caused by artificial application of stress waves [7], and that in the secondary crack nucleation sites AE waves should be intense enough because the sites are much closer to the main crack front. Therefore, existence of AE waves is considered to become a dynamic factor

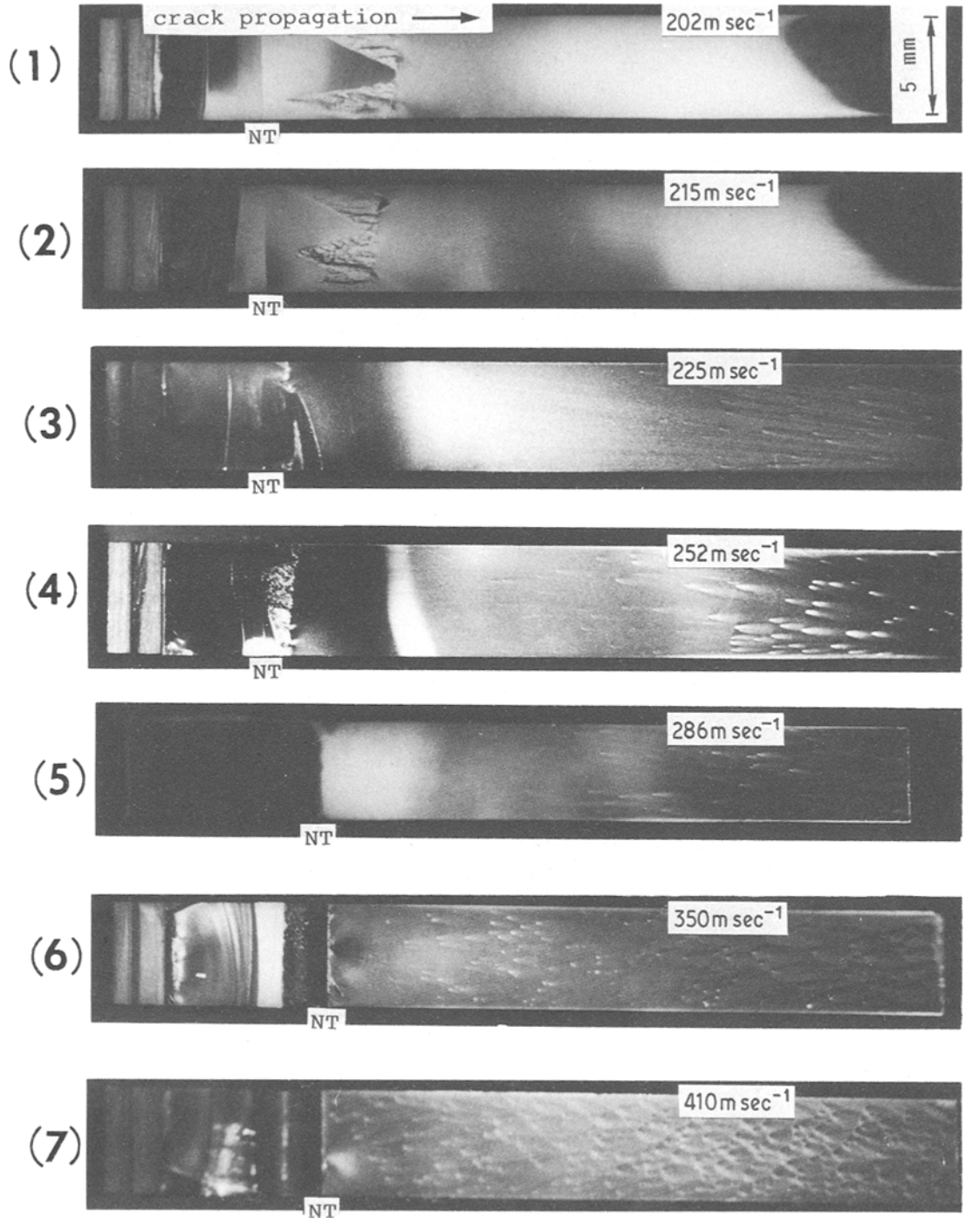

Figure 7 Optical photographs of fracture surfaces of the specimens loaded under various conditions. NT means positions of the initial notch front. The kinds of notches and crosshead speeds adopted were as follows; (1) fatigue crack, 1 mm min^{-1}, (2) fatigue crack, 10 mm min^{-1}, (3) fatigue crack, 100 mm min^{-1}, (4) fatigue crack, 500 mm min^{-1}, (5) V-shaped notch, 100 mm min^{-1}, (6) 2 mm diameter drill-hole notch, 100 mm min^{-1} and (7) 3 mm diameter drill-hole notch, 100 mm min^{-1}.

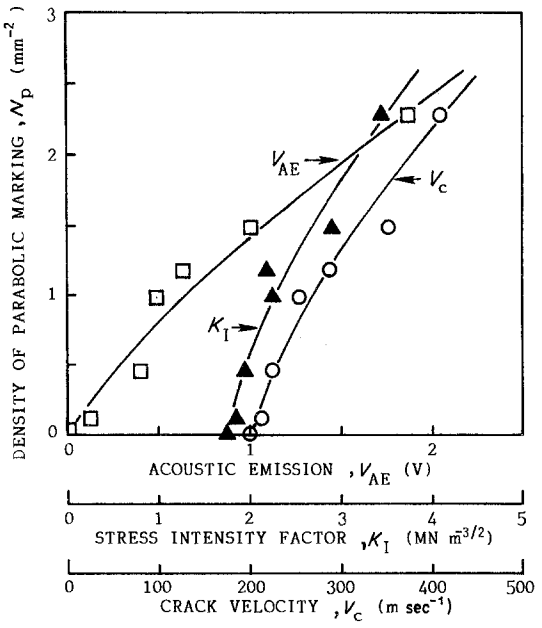

Figure 8 Correlations between amplitude of AE signals, mode I stress intensity factor, crack velocity and density of parabolic markings which were obtained from the specimens shown in Fig. 7.

as coupled with the static factor in the secondary crack nucleation process.

As a concluding remark, the following picture may be drawn for a formation mechanism of secondary cracks in PMMA. As a "static factor", there exist defects of several kinds such as microvoids, heterogeneity in microscopic density distribution, silicon compounds, and other foreign materials introduced during material processing courses. These randomly included stress raisers form potential sites for nucleation of the secondary fracture. With increasing stress intensity and fracture velocity of the main crack, amplitude of AE waves becomes higher (see Fig. 5). Because AE waves should have both longitudinal and transverse components, not only mode I but also mode II or III stress intensity may result from the waves, causing a dynamic perturbation in the magnitude of total stress intensity ahead of the main crack front. When fracture velocity attains some 200 m sec^{-1}, the perturbed stress intensity will become high enough to activate the static factor, inducing the secondary crack initiation. The higher the amplitude of the stress waves is, the higher the formation probability for the secondary fracture would be. Thus, by the combination of these static and dynamic motives, the formation mechanism of secondary cracks and the density of parabolic markings seem to be reasonably explained.

Acknowledgements

The authors express their sincere thanks to Professor T. Suhara and Mr S. Fukuda for useful comments on the EPMA study. The experimental assistance of Messrs N. Komatsu and T. Mada is also acknowledged.

References

1. J. K. KIES, A. M. SULLIVAN and G. R. IRWIN, *J. Appl. Phys.* **21** (1950) 716.
2. F. ZANDMAN, "Etude de la Déformation et de la Rupture des Matieres Plastiques" (Publications Scientifiques et Techniques de Ministère de l'Air, Paris, France, 1954).
3. I. WOLOCK and S. B. NEWMAN, "Fracture Processes in Polymeric Solids", edited by B. Rosen (Wiley and Sons, New York, 1964) p. 236.
4. J. P. BERRY, *ibid.* p. 195.
5. S. B. NEWMAN and I. WOLOCK, *J. Appl. Phys.* **29** (1958) 49.
6. B. COTTERELL, *Int. J. Fract. Mech.* 4 (1968) 209.
7. K. TAKAHASHI, S. KUNIEDA and A. SUZUKI, *Jpn. J. Appl. Phys.* **11** (1972) 1233.
8. R. P. KUSY and D. T. TURNER, *Polymer* **18** (1977) 391.
9. M. J. DOYLE, *J. Mater. Sci.* **17** (1982) 204.
10. P. MANOGG, *Glastech. Berichte* **39** (1966) 323.
11. K. TAKAHASHI and S. HYODO, *J. Macromol. Sci.-Phys.* **B19** (1981) 695.

Received 7 June
and accepted 21 July 1983